November 2014

Effect of Chemotherapeutic Treatment Schedule on a Tissue Transport Model

Dan E. Ganz
University of Massachusetts Amherst

Effect of Chemotherapeutic Treatment Schedule on a Tissue Transport Model

A Thesis Presented

by

DAN E. GANZ

Submitted to the Graduate School of the
University of Massachusetts Amherst in partial fulfillment
of the requirements for the degree of

MASTER OF SCIENCE IN CHEMICAL ENGINEERING

September 2014
Chemical Engineering

Effect of Chemotherapeutic Treatment Schedule on a Tissue Transport Model

A Thesis Presented

by

DAN E. GANZ

Approved as to style and content by:

_____
Neil S. Forbes, Chair

_____
David Ford, Member

_____
Joseph Jerry, Member

_____

T.J. (Lakis) Mountziaris, Department Head

Department of Chemical Engineering

DEDICATION

To Zvi, Aura, Adi, and Michal Ganz, my amazing family.

ACKNOWLEDGEMENTS

This Masters would not have been possible without the guidance and support of Dr. Neil Forbes and his research group. I am thankful for his advice throughout my graduate work. I would also like to thank my committee members, Dr. David Ford Dr. Joseph Jerry, for their feedback.

ABSTRACT

EFFECT OF CHEMOTHERAPEUTIC TREATMENT SCHEDULE ON A TISSUE TRANSPORT MODEL

SEPTEMBER 2014

DAN E. GANZ, B.SC., UNIVERSITY OF MASSACHUSETTS AMHERST

M.S. CH.E., UNIVERSITY OF MASSACHUSETTS AMHERST

Directed by: Professor Neil S. Forbes

Current chemotherapeutic treatment schedule prediction methods rely heavily on PK/PD-based models and overlook the important contribution of tissue-level transport and binding. Tissue-level transport and binding phenomena are essential to understanding drug delivery and efficacy in tumors. Drugs with desirable PK/PD properties often fail *in vivo* due to poor tissue-level transport. We developed an *in silico* method to predict the effect of treatment schedule on efficacy that couples PK/PD with tissue-level transport. Treatment schedules were implemented on theoretical drugs with different PK/PD and transport properties. For each drug with a given clearance rate, diffusivity, and binding, treatment schedules consisting of one to 20 doses were simulated. Results show that at binding constants around one, high diffusivities, and high clearance rates, implementation of a treatment schedule becomes more significant. At low clearance rates, regardless of tissue-level transport and binding, one dose was predicted to be most efficacious. Tissue Drug Exposure (TDE) was shown to be to a crucial factor for treatment schedule efficacy. Efficacy was improved by increasing TDE. Implementation of a treatment schedule with more doses than one curbed the effect of poor retention with drugs. This

model investigates the effect of treatment schedule on a tissue transport model and shows implementation of a proper dosing regimen is crucial to maximize TDE and chemotherapeutic efficacy.

TABLE OF CONTENTS

Page

LIST OF TABLES

LIST OF FIGURES

Figure **Page**

CHAPTER 1

INTRODUCTION

Chemotherapy is an extremely common cancer therapy worldwide. It is estimated that in 2014, 1.6 million people in the US alone will be diagnosed with cancer (Howlader et al., 2011). Of those patients, approximately 20% will receive chemotherapy (Kolodziej et al., 2011). Predicting a dosing regimen of chemotherapy is critical to maximize effectiveness of the treatment. Intracellular area under the concentration-time curve (AUC) has been shown to be an effective predictor of chemotherapeutic drug efficacy (Nagai & Ogata, 1997). The classic "more is better" approach of increasing the maximum tolerable dose (MTD) can only go so far in improving chemotherapeutic efficacy for cancer patients (Takimoto, 2009). Currently, optimal treatment schedules are primarily predicted via mouse models. Mouse models can be extremely expensive and time-consuming. An average of $330,000 is needed just to adequately test a single potential drug candidate in mouse models. In addition, 80% of drugs that are predicted to be effective in mice fail when tested in humans (Perrin, 2014). Hence, accurate *in silico* models are desirable to reduce cost and time spent in animal models.

Many drugs that are successful *in vitro* fail *in vivo*. This is because drugs are not able to effectively penetrate the tumor, as opposed to the drug having poor efficacy on the tumor cells themselves (el-Kareh & Secomb, 1997; Minchinton & Tannock, 2006; Toley, Tropeano Lovatt, Harrington, & Forbes, 2013; Tredan, Galmarini, Patel, & Tannock, 2007; Venkatasubramanian, Henson, & Forbes, 2008). Drug clearance rate is crucial to efficacy. Tissue-level transport (diffusion) and binding are also crucial to predict a drug's ability to penetrate vasculature and reach the tumor. These mass transfer effects play a

critical role in drug penetration and retention in cancerous tumors. A drug's ability to penetrate a tumor is determined by its diffusivity and its ability to be retained inside the tumor is dependent upon its binding properties. Drug diffusion and retention are neglected in pharmacokinetic and pharmacodynamic (PK/PD)-based models yet have considerable effect on efficacy. Drug bound to tissue induces cancer cell death. A low diffusivity can prevent effective penetration of the drug into the tumor region from the blood vessel. With a low diffusivity, the drug can be cleared from the body before enough drug reaches the tumor tissue. High diffusivity reduces and limits retention. Even with desirable pharmacokinetic and pharmacodynamic properties, drugs can fail *in vivo* due to poor tissue level transport (Toley et al., 2013). A model to predict optimal chemotherapeutic regimens must: (a) incorporate pharmacokinetics/pharmacodynamics and (b) include mass transfer effects such as tissue-level transport and binding kinetics.

In silico models that predict treatment schedules are reported in (Carlson & Sikic, 1983; El-Kareh & Secomb, 2003; Jones, Secomb, Dewhirst, & El-Kareh, 2014; Levasseur, Slocum, Rustum, & Greco, 1998). El-Kareh et al successfully models pharmacodynamics of Cisplatin at the cellular level with varying exposure times. The model incorporates uptake kinetics and intracellular binding while examining survival versus exposure time. Jones at al presents a model that predicts cancer cell response to combinations of chemotherapeutic drugs. It also models at the cellular level and incorporates intracellular uptake and cytotoxicity. Jones et al state in their study that the limitations of extracellular transport were not considered. Like El-Kareh et al, Levasseur et al investigates effect of exposure time on chemotherapeutic antitumor activity. Carlson et al investigate the effect of continuous injection versus bolus injection on systemic

toxicity and antitumor efficacy. To the best of our knowledge, no one has investigated the effect of treatment schedule on a tissue transport model.

In this study, plasma concentration of a given chemotherapeutic drug is at a maximum immediately upon IV bolus administration. The plasma concentration of the drug decreases over time due to absorption and metabolism (Lin & Lu, 1997). The rate of clearance of the drug from the body is determined by the half-life. AUC is kept constant. The drug arrives to the tumor site and penetrates into tumor tissue via diffusion. Once in the tissue, the drug can bind on to and then off of cancer cells at a specified ratio determined by the binding constant. If the drug binds to a cancer cell, the drug can then kill the cell. The cancer cells have a specified maximum rate of death in response to the drug. The drug can also saturate the tissue at a certain concentration.

CHAPTER 2

METHODOLOGY

2.1 Model Formulation

Three dimensionless simultaneous time-dependent partial differential equations that balance free drug (C), drug bound to cells (B), and the local fraction of viable cancer cells (N) describe the phenomena discussed in Chapter 1.

The following system of partial differential equations were solved using the finite element method:

$$\begin{aligned}\frac{\partial C}{\partial t} &= D\frac{\partial^2 C}{\partial x^2} - k_{on}C + k_{off}B \\ \frac{\partial B}{\partial t} &= k_{on}C - k_{off}B \\ \frac{\partial N}{\partial t} &= -\mu_D^{\max}\frac{C+B}{K_m + C + B}\end{aligned} \qquad \text{Equation 1}$$

where k_{on} is the parameter of binding of drug on to cells, k_{off} is release of drug off of cells, μ_D^{max} is the maximum rate of cell death, and K_m is the cell death saturation. Four main mechanisms and six key parameters contribute to this model: diffusivity (D), cell binding (k_{on}, k_{off}), cell death (μ_D^{max}, K_m) and clearance ($t_{1/2}$). The binding constant (R) is defined as k_{on} / k_{off}. The boundary and initial conditions are:

$$@\, t = 0; C_0 = B_0 = 0; N_0 = 1 \qquad (1)$$

$$@\, x = 0; C = C_0 e^{\frac{t}{t_{1/2}}} \qquad (2)$$

$$@\, x = L; \frac{\mathrm{dC}}{\mathrm{dx}} = \frac{\mathrm{dB}}{\mathrm{dx}} = \frac{\mathrm{dN}}{\mathrm{dx}} = 0 \qquad (3)$$

where $t_{1/2}$ is the half-life of the drug and L is the width of the tissue. It was assumed that the tissue here is linear and one-dimensional because of negligible curvature. At the proximal edge of the tissue (x=0), the interface with the blood channel, the concentration of drug was equal to the concentration in the blood. A Neumann boundary condition of zero flux due to symmetry is imposed at the distal edge of the tissue (x=L).

The boundary condition at the proximal edge of the tissue included a step change to simulate a treatment schedule. Keeping exposure time constant, for a given drug with mass transport and PK parameters, the only variable manipulated in the model was amount of doses. The exposure time was split into equal time steps for dosing administration. Correspondingly, AUC was kept constant. Doses administered via IV bolus are immediately dispersed in plasma upon administration. Thus, the concentration of drug at the proximal edge of the tumor tissue was equal to the concentration of drug in the plasma at any given time.

2.2 Data Analysis

A wide range of theoretical drugs with varying diffusivities, binding constants, and clearance rates were created to analyze the effect of treatment schedule on efficacy. Efficacy was measured by fraction of viable cells killed. Depending on protocol, chemotherapy treatment can last hours or days. 72 hours was found to be a reasonable treatment period. Theoretical drugs with static parameters (Table 1) and variable parameters (Table 2) were analyzed for efficacy over a range of treatment schedules. The

static parameters investigated match closely to those of Doxorubicin (Toley et al., 2013). Variable drug tissue transport and PK parameters included the diffusivity (D), the binding constant (R), and the clearance rate (pharmacokinetic half-life, $t_{1/2}$). The effect of treatment schedule was then investigated on the drugs with different tissue transport and PK parameters. Treatment schedules of up to and including 20 doses were investigated. For a drug with a given diffusivity, binding constant, and clearance rate, all treatment schedules were simulated for efficacy that was determined by fraction of tumor cells killed. Tissue Drug Exposure (TDE) was measured by numerically integrating the area under the curve of bound drug using Simpson's Rule. These simulations were executed for all possible combinations of tissue transport and PK parameters. Static parameters (Table 1) remained the same for every drug.

Table 1 Variable (investigated) parameters for theoretical drugs

Symbol	Description	Units	Range
D	Diffusivity	m^2s^{-1}	10^{-18} to 10^{-2}
R (k_{on}/k_{off})	Binding Constant	dimensionless	10^{-4} to 10^{-4}
$t_{1/2}$	Clearance half-life	hrs	0.5, 5, 15

Table 2 Static parameters for theoretical drugs

Symbol	Description	Units	Value	Reference
L	Length	m	800×10^{-6}	(Less, Skalak, Sevick, & Jain, 1991)
C_0	Dose Administered	mol m^{-3}	2×10^{-2}	(Tang et al., 2014)
K_m	Saturation constant	mol m^{-3}	1.66×10^{-3}	(Toley et al., 2013)
μ_D^{max}	Maximum rate of cell death	s^{-1}	3.89×10^{-5}	(Toley et al., 2013)

Two parameters were created in order to quantitatively analyze efficacy and optimal treatment schedule. The One Dose-Twenty Dose (ODTD) and Maximum Marginal Change (MMC) were used to determine whether an implementation of more than one dose would improve efficacy and where the optimal dose lies, respectively. The ODTD was defined as the 1-dose killing percentage subtracted from 20-dose killing percentage. The ODTD parameter is used to determine whether administering more than one dose has a significant effect. If the ODTD was found to be greater than 0.02, giving more than one dose is found to be more efficacious. One dose is most efficacious if the ODTD is below than 0.02. A higher ODTD corresponds to a drug that is more efficacious with more doses. The MMC was the dose at which there exists a 1% difference from the 20 dose killing percentage. The dose at which the MMC is 0.01 was found to be the optimal dose.

CHAPTER 3

RESULTS

Implementation of treatment schedules significantly changed efficacy for drugs of differing transport parameters (Figure 1). A treatment schedule with more doses improved efficacy for the drug with higher diffusivity and lower binding constant (Figure 1A), and decreased efficacy for the drug with lower diffusivity and higher binding constant (Figure 1B).

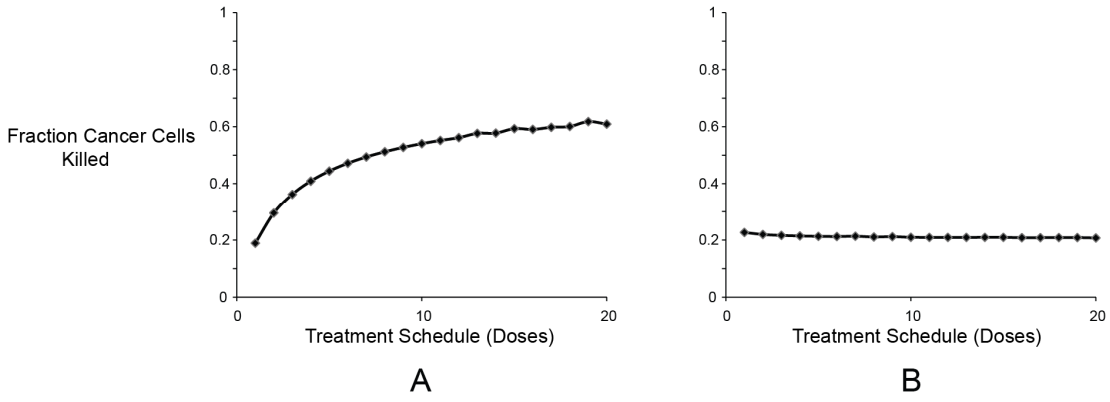

Figure 1. Fraction of cancer cells killed at treatment schedules consisting of 1 to 20 doses in a 72 hour time period. Half-life is kept constant at 0.5 hours. A: Drug with diffusivity of 10^{-8} m^2/s and binding constant of 10^{-2}. B: Drug with diffusivity of 10^{-12} m^2/s and binding constant of 10^2.

The ODTD determined whether efficacy was significantly improved with more than one dose. Drugs with identical clearance rates but different tissue transport parameters R and D had significantly different ODTD values (Figure 2, right). With a more positive value of ODTD, a greater improvement in efficacy is observed with a given drug. At a half-life of 0.5 hours and across all binding constants, drugs with a higher diffusivity exhibited a higher ODTD. With higher diffusivity, tissue penetration increases but retention decreases, and thus implementation of a treatment schedule with more doses improves efficacy by curbing this phenomenon. Across all diffusivities greater than 10^{-10} m^2/s, drugs with a binding constant of 1 exhibited the greatest ODTD. At the diffusivity range, drugs with binding constants less than 1 exhibited greater ODTD values than drugs with binding constants above 1. At a higher half-life of 5 hours, ODTD was greatest for drugs with high diffusivities and low binding constants. High diffusivity and low binding constant results in low tissue retention and poor drug binding. Hence, implantation of a treatment schedule with more doses significantly improves efficacy. Implementation of a treatment schedule with more doses can only go so far for drugs with poor retention. Hence, ODTD is optimal for drugs with binding constant of one. At even lower binding constant (10^{-4}) retention becomes more significant and implementation of treatment schedule becomes not as effective implementing a treatment schedule for drugs of high diffusivity and binding constant one. Decreasing the drug clearance rate curbs the low retention/poor binding effect and hence ODTD decreases as half-life increases.

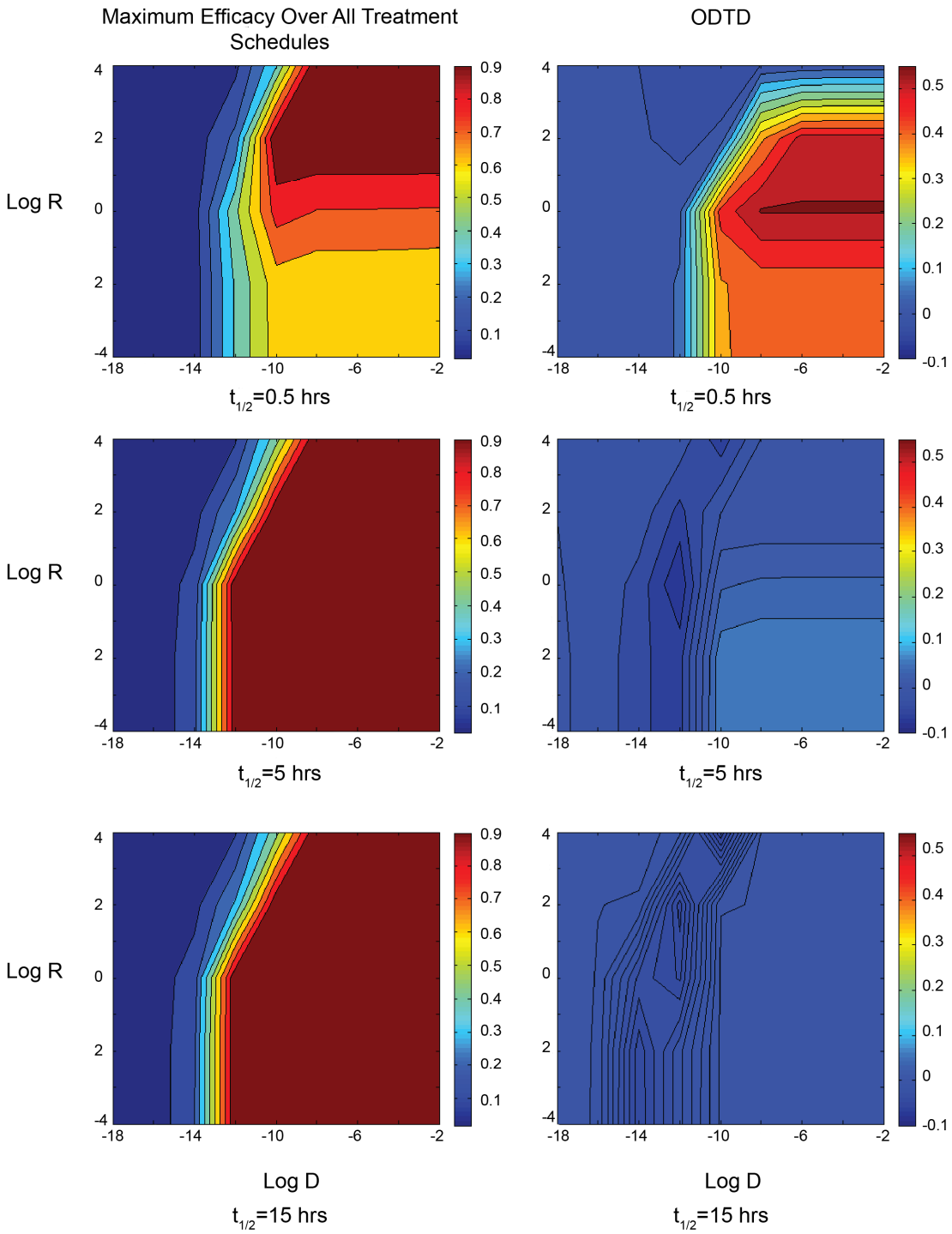

Figure 2. ODTD for two half-lives keeping *D* and *R* fixed. A) a half-life of 0.5 hours and diffusivity of 10^{-10} m^2/s. B) a half-life of 0.5 hours at binding constants of 1 and 100. C) a half-life of 5 hours and diffusivity of 10^{-10} m^2/s. D) a half-life of 5 hours at binding constant of 1.

The optimal efficacy across all treatment schedules (Figure 2, left) was dependent on both tissue transport and PK/PD drug properties. Drugs with a half-life of 0.5 hours exhibited high efficacy at high diffusivities and high binding constants. However, drugs with low binding constants and high diffusivities were not as efficacious as those with higher binding constants and high diffusivities. This, again, could be attributed to poor retention of drug in tumor tissue. Similar to ODTD, at all binding constants efficacy also increased across drugs with higher diffusivity. Efficacy increased due to implementation of treatment schedule. Drugs with lower clearance rates (higher half-lives) did not exhibit poor efficacy at high diffusivities and low binding constants. A low clearance rate improved retention of drug in tumor tissue. Across all binding constants and diffusivities, drugs with higher half-lives had a greater efficacy.

The trends for treatment schedules of up to 20 doses over 72 hours significantly changed for drugs of different tissue transport and PK/PD properties (Figure 3). Dosing regimens of these theoretical drugs could be predicted. No optimization is needed for treatment schedules as a simple trend exists for the search space investigated.

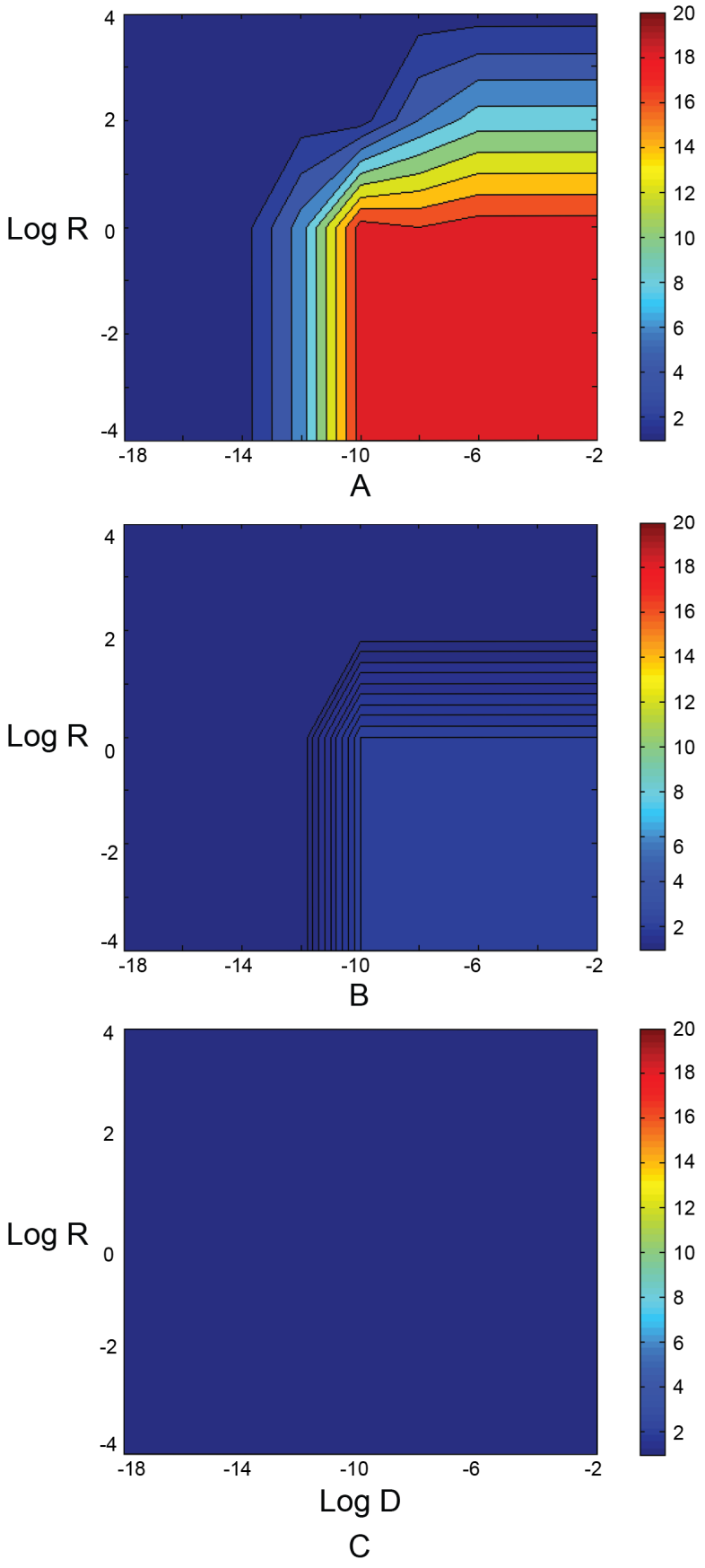

Figure 3. Treatment schedule (number of doses) contour maps for drugs with a half-life of A: 0.5 hours, B: 5 hours, and C: 15 hours.

At a half-life of 0.5 hours, a treatment schedule of more doses is most beneficial for drugs with high diffusivity and low binding constants (Figure 3a). At high diffusivity and low binding constants, drugs are not retained effectively in tumor tissue. This is true especially with high clearance rates. Retention can be improved by increasing the binding constant and thus drugs with higher binding constants at high diffusivity do not benefit from more doses. Drugs with low diffusivity retain better in tumor tissue, and thus such drugs also do not benefit from more doses across all binding constants. At binding constants less than and including one, more doses resulted in significant improvement in efficacy (ODTD≥0.02) at diffusivities greater than and including 10^{-12} m^2/s. For drugs with a binding constant of 10^2, there was significant improvement in efficacy with more than one dose for drugs with diffusivities greater than and including 10^{-8} m^2/s. For drugs with a binding constant of 10^4, there was no significant improvement in efficacy with more than one dose across all diffusivities.

Drugs with lower clearance rates exhibited less benefit from a treatment schedule consisting of more doses (Figure 3b). Similar to drugs with a half-life of 0.5 hours, drugs with a half-life of 5 hours only benefited from more doses at high diffusivities and low binding constants. These drugs still exhibit poor retention and hence benefit from more doses. Drugs with binding constants less than and including one, two doses resulted in significant improvement in efficacy at diffusivities greater than and including 10^{-10} m^2/s. At binding constants greater than one, no improvement in efficacy with more than one dose was observed over all diffusivities.

Drugs with the lowest clearance rates, at a half-life of 15 hours, exhibited no improvement in efficacy with more than one dose over all binding constants and

diffusivities (Figure 3c). A drug with a low clearance rate is retained in the blood for a longer period of time. This phenomenon curbs the poor tissue retention effect exhibited with drugs of higher clearance rates. Treatment schedule recommendations were summoned from the model (Figure 4).

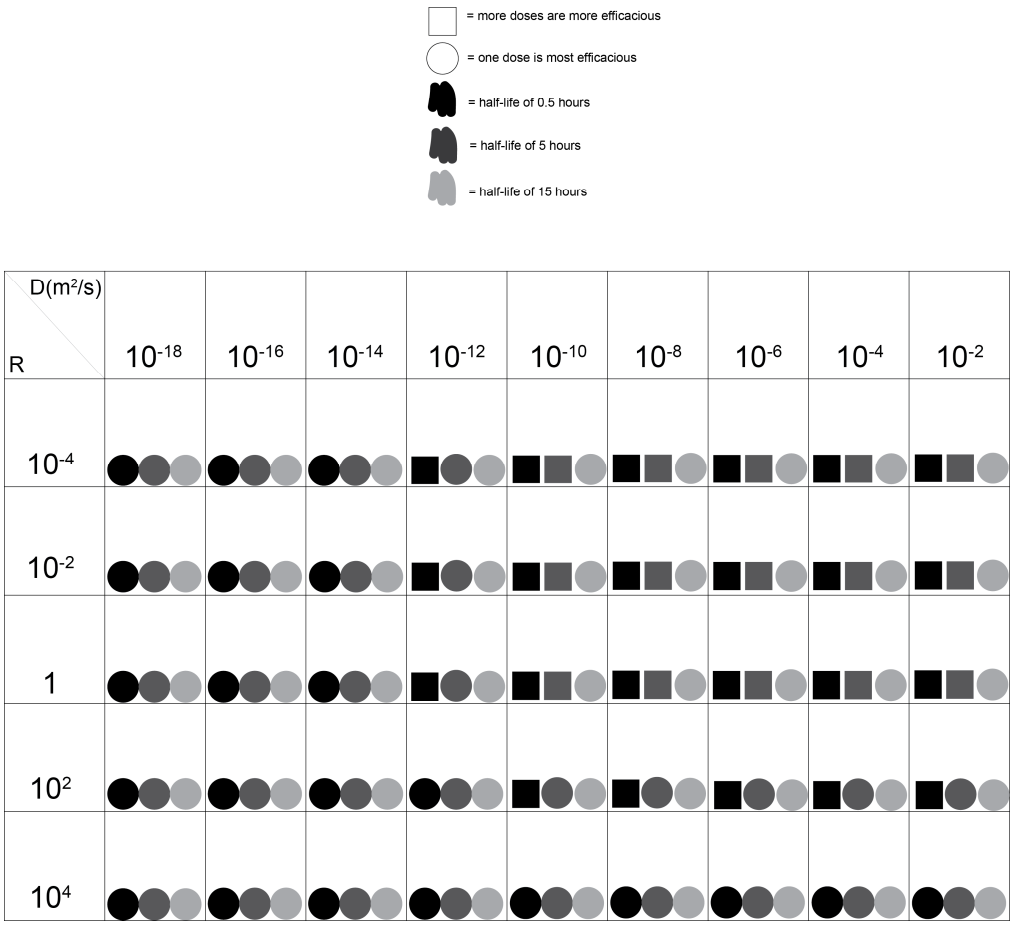

Figure 4. Overall trend map of optimal treatment schedules for drugs of a given half-life and various tissue transport properties.

Treatment schedule efficacy was directly correlated to TDE (Figure 5). Efficacy (Figure 5a) and TDE were calculated for drugs with different tissue transport parameters and the same clearance rate for treatment schedules consisting of two and ten doses. TDE

was calculated for drug bound to tumor cells (Figure 3b). The relative improvement (percent improvement in killing) was taken between each treatment schedule. There was found to be a correlation between the percent improvement in killing and TDE, with a Pearson product-moment correlation coefficient of 0.99. With higher drug exposure to tumor tissue, efficacy increased. In cases where administering more doses was found to have no improvement on efficacy, TDE had no increase. Treatment schedule can improve TDE with constant AUC when incorporating tissue transport, thus improving efficacy.

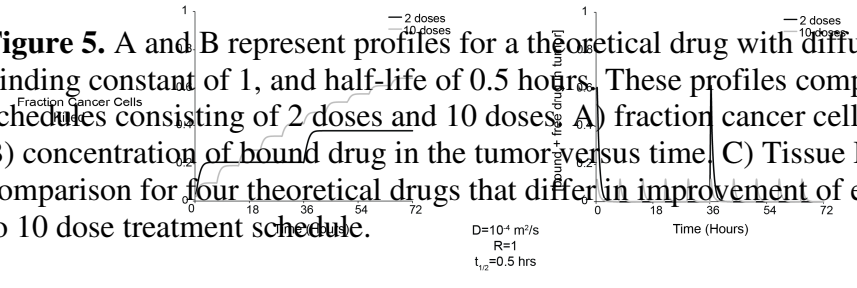

Figure 5. A and B represent profiles for a theoretical drug with diffusivity of 10^{-4} m^2/s, binding constant of 1, and half-life of 0.5 hours. These profiles compare treatment schedules consisting of 2 doses and 10 doses. A) fraction cancer cells killed versus time. B) concentration of bound drug in the tumor versus time. C) Tissue Drug Exposure (TDE) comparison for four theoretical drugs that differ in improvement of efficacy from 2 dose to 10 dose treatment schedule.

CHAPTER 4

CONCLUSION AND FUTURE WORK

This study presents a tissue transport model that illustrates the effect of treatment schedule on chemotherapeutic antitumor efficacy. Previous studies show tissue level transport plays a key role in penetration and retention of drug (Toley et al., 2013). At high diffusivities, low binding constant, and low half-life, a drug is quickly cleared from the body and penetrates the tumor well but is not retained. A treatment schedule consisting of more doses helps improve efficacy by increasing TDE (Figure 5). At high diffusivities and high binding constants for all half-lives, a drug penetrates the tumor well and is retained. Implantation of treatment schedule on such drugs has no significant improvement on efficacy (Figure 2). At higher half-lives (15 hours), drug is cleared slowly from the body and has more time be in contact with the tumor. Regardless of diffusivity or binding constant, implementation of treatment schedule consisting of more than one dose had no improvement on efficacy. Based on this model, drugs that exhibit higher clearance rates have greater improvement in antitumor efficacy using a treatment schedule with more than one dose. The model developed here is a useful tool to predict optimal treatment schedules. Doxorubicin, an established chemotherapeutic drug, currently has a 72-hour treatment schedule with 12 doses. This model predicts the optimal treatment schedule would be 10 doses over 72 hours. Thus, compared with the drug of which the model static parameters were taken, this model predicted accurately the dosing scheme of Doxorubicin. With this model the optimal efficacy, optimal treatment schedule, and improvement from one dose can thus be predicted. From this study, we can

conclude that it is essential to also take tissue transport phenomena into account as well as PK/PD for *in silico* treatment schedule models.

There are several components that could be added to the model to improve accuracy of prediction. First, unequal dosing regimens could be investigated. This could perhaps further improve efficacy. Second, tumor growth could be incorporated into the model. Over the time period investigated, it was assumed tumor cells did not regenerate. Adding such a component to the model can further improve treatment schedule prediction accuracy.

APPENDIX

MATLAB CODE FOR TISSUE TRANSPORT MODEL AND INVESTIGATION OF TREATMENT SCHEDULES FOR THEORETICAL DRUGS

optim.m

```
%THIS M FILE INVESTIGATES ALL THEORETICAL DRUGS
%the m file runs Looping, func, conc_blood, and nonline m files

ndose=20; %input treatment schedules to investigate here (1 to ndose treatment schedules will
be investigated)

%all possible combinations of Dfact, Rfact, and Thalf will be investigated

Dfact=[1e-6,1e-4,1e-2,1,1e2,1e4,1e6,1e8,1e10]; %diffusivities to investigate
Rfact=[1e-4,1e-2,1,1e2,1e4];%binding constants to investigate
Thalf=[0.5,5,15];%half-lives to investigate

%create for-loops to investigate all possible combinations

out=zeros(ndose, length(Dfact)*length(Rfact)*length(Thalf));
counter = 0;
for i = 1:length(Dfact)
   for j = 1:length(Rfact)
      for n = 1:length(Thalf)
         counter = counter+1;
         for M=1:ndose
               out(M, counter)=Looping(M, Thalf(n), Dfact(i), Rfact(j));
               disp(['Thalf ', num2str(n)]);
               disp(['Dfact ', num2str(i)]);
               disp(['Rfact ', num2str(j)]);
         end
      end
   end
end
```

Looping.m

```
function loop=Looping(dose,thalf, dfact, rfact)
% THIS CODE SOLVES THREE SIMULTAEOUS PDE'S FOR CONCENTRATION OF FREE
DRUG,
% BOUND DRUG, AND LIVE CELLS WITHIN TISSUE

%---- Discretization Parameters----------
T = 72; % Total experiment time (hours)
dose=10; %manually input treatment schedule (number of doses) here to investigate one
treatment schedule
dfact=1e8;%manually input diffusivity here to investigate one treatment schedule
rfact=1e4;%manually input binding consant to investigate one treatment schedule
thalf=5;%manually input half-life here to investigate one treatment schedule
ndose=dose; %number of drug doses
Nt = 200; % Number of bins in time;
N = 50; % Number of bins in x (distance)


%-----------------------------------------------
h = 1/ N; % Non dimensional step size in space

%Loop the entire structure to investigate the dependence of a parameter
Size = 1;
Result = zeros(4,Size);
for Pass=1:Size

% GENERATING INITIAL CONDITION VECTOR
% Setting all initial values to zero, except live cell density, which is
% set to 1 at time t=0
X0 = zeros(((3*N)+2),1);
for i = (2*N)+2 : (3*N)+2
    X0(i,1) = 1;
end


%Manipulations

Dfact = dfact;
Mufact = 1;
Konfact = 1;
Rfact = rfact;

A0fact = 1;   %10^(Pass-11);

%------- Solution Parameters
%-----------------------------------------------------------------

L = 800e-6; % Length of domain (m)

D = Dfact*(1e-12); % Diffusivity of Dox (m2/s)
```

```
kon = 1.00 * Konfact; % Forward reaction rate constant (1/s)

R = 1 * Rfact; % Equilibrium constant = kon/koff

koff = kon/R; % Reverse reaction rate constant (1/s)

Thalf = thalf;
%Thalf = .2; %half-life (hours, used in conc_blood)

A0 = 2e-2 * A0fact; % Maximum drug concentration. Value in parenthesis is in uM. It is converted
to mol/m3

Km = (1.66) * (1e-3); % drug saturation constant. Value in parenthesis is in uM. It is converted to
mol/m3

Mudmax = (0.14) * Mufact / 3600; % Max death rate. Value in parenthesis is in 1/hr. It is
converted into 1/s

frac = 1; % Contribution of free drug to killing cells; 0<frac<1

Ratio=(L.*L)/D;

dt = ((T*3600)/Nt)*(1/Ratio); % Non dimensional step size in time




%-----------------------------------------------------------
% DIMENSIONLESS VARIABLES

KON = kon*Ratio;
KOFF = koff*Ratio;
T0 = Ratio;
MU = Mudmax*Ratio;
Q = Km/A0;
%-----------------------------------------------------------


%-- Pre-defining Mass Matrix and Vectors as Zeros --------

A = zeros ((3*N)+2);



%-----------------------------------------------------------
```

```
%-- Creating Mass Matrix A --------

f = 1/(h^2); % for convenince

%Row 1
A(1,1) = (-2*f) - KON;
A(1,2) = f;
A(1, N+2) = KOFF;



%Row N
A(N,N-1) = 2*f;
A(N,N) = (-2*f) - KON;
A(N,N+N+1) = KOFF;

%Rows 2 to N-1
for i = 2:N-1
    A(i,i-1) = f;
    A(i,i) = (-2*f) - KON;
    A(i,i+1) = f;
    A(i,i+N+1) = KOFF;
end

%Row N+1
A((N+1),(N+1)) = -KOFF;


%Rows N+2 to N+N+1
for i = 1:N
    A(N+1+i,i) = KON;
    A(N+1+i,i+N+1) = -KOFF;
end
%------Finished creating matrix A----
%----------------------------------------


%Initializing Solution Matrix---
C = zeros(((3*N)+2),Nt); % Final Solution Matrix
Y = zeros(((3*N)+2),1);


% MAIN SOLVER-------------------------------------------
sol = X0;

for i = 1:Nt
    t = (i-1)*dt; %Nondimensionalized time
    X = sol;
    sol = fsolve(@(Y) func(X,Y,f,t,dt,T0,A,N,MU,Q,KON,frac,ndose,Thalf), X);
    C(:,i) = sol;
end
%-----------------------------------------------------
```

```
%-----Extracting individual components from solution-------
conc_A = zeros(N+1,Nt);

conc_A(2:N+1,:) = C(1:N,:);

for i = 1:Nt
    t = (i)*dt;
    conc_A(1,i) = conc_blood(t,T0,ndose,Thalf);
end


conc_B = C((N+1):((2*N)+1),:);

conc_tot = conc_A + conc_B;

conc_live = C((2*N)+2:(3*N)+2,:);


%---- creating axes for plots
t_axis = T/Nt:T/Nt:T;
x_axis = 0:h:1;


% %---- PLOTS --------

subplot(2,3,1)
plot (x_axis,conc_A);
xlabel ('distance');
ylabel ('Conc of free drug');

subplot(2,3,2)
plot (x_axis,conc_B);
xlabel ('distance');
ylabel ('Conc of bound drug');

subplot(2,3,3)
plot (x_axis,1-(conc_live));
xlabel ('distance');
ylabel ('dead cell concentration');

subplot(2,3,4)
plot (t_axis,mean(conc_A));
xlabel ('time (hrs)');
ylabel ('average free drug conc');

subplot(2,3,5)
plot (t_axis,1-mean(conc_live));
xlabel ('time (hrs)');
ylabel ('average dead cell conc');
```

```
subplot(2,3,6)
plot (t_axis,mean(conc_B));
xlabel ('time (hrs)');
ylabel ('average bound drug conc');

%write excel data here
xlswrite('t_axis', t_axis);
xlswrite('x_axis', x_axis);
xlswrite('mean(conc_B)', mean(conc_B));
xlswrite('mean(conc_A)', mean(conc_A));
xlswrite('conc_B', conc_B);
xlswrite('conc_A', conc_A);
xlswrite('1-conc_live', 1-conc_live);
xlswrite('1-mean(conc_live)', 1-mean(conc_live));
% Can display values here
% ratio = conc_live(0.8*N,Nt) / conc_live(0.2*N,Nt);
%
% %disp([length(x), x(length(x),5), x(length(x),6), ratio])
% disp(' ')
% disp(num2str(Pass));
% disp(['survival ', num2str(mean(conc_live(:,Nt)))]);
% disp(['proximal ', num2str(conc_live(0.2*N,Nt))]);
% disp(['distal ', num2str(conc_live(0.8*N,Nt))]);
% disp(['ratio ', num2str(ratio)]);
%
% saveas(gcf,['Exp_RD2_' num2str(Pass+5)]);
%
% Result(1,Pass)=mean(conc_live(:,Nt));
% Result(2,Pass)=conc_live(0.2*N,Nt);
% Result(3,Pass)=conc_live(0.8*N,Nt);
% Result(4,Pass)=ratio;
%
% end;
% loop=mean(conc_live(:,Nt));


end
```

Func.m

```
function c = func(X,Y,f,t,dt,T0,A,N,MU,Q,KON,frac,ndose,Thalf)

I = eye ((3*N)+2);

M = (I - (dt*A));

b = zeros (((3*N)+2),1);

A1=X(1,1)/f;
A2=X((N+1),1)/KON;

b(1,1) = f*conc_blood(t+dt,T0,ndose,Thalf);

b((N+1),1) = KON*conc_blood(t+dt,T0,ndose,Thalf);


c = M*Y - X - (dt*b) - (dt*Nonlin(t,dt,T0,Y,MU,Q,frac,N,ndose,Thalf));
```

Conc_blood.m

```
function c = conc_blood(t,T0,ndose,Thalf)

T=72; %total experiment time
M=ndose;%number of doses

delt=T/M;%interval between each dose (hours)

K = 0.693/Thalf; % 1/hrs

t_dim = t.*T0/3600;% time (hours)


C0=1/M; %concentration of each administered

cd=zeros(M,1); %create concentration profiles for each dose
for i=1:M
   cd(i,1) =C0*exp(-K.*(t_dim-((i-1).*delt))); % Normalized boundary condition
end
c=0;

%implement dose at each interval
if t_dim <= delt %first dose implemented
   c=cd(1,1) ;
end
```

```
for i=M:-1:2 %doses 2 to ndose implementation


   if t_dim > (i-1)*delt

      for j=1:(i)
         c=cd(j,1)+c;
      end
      break;
   end
end
```

Nonlin.m

```
function c = Nonlin(t,dt,T0,X,MU,Q,frac,N,ndose,Thalf)



CA = X(1:N);
CB = X(N+1:(2*N)+1);
If = X(((2*N)+2):((3*N)+2));

vect = zeros(((3*N)+2),1);


Ceff = (frac*conc_blood(t+dt,T0,ndose,Thalf)) + CB(1,1);
vect((2*N)+2,1) = -MU * (Ceff/(Q + Ceff)) * If(1);

for i = 2:(N+1)

   Ceff = (frac*CA(i-1) + CB(i));

   vect((2*N)+1+i,1) = -MU * (Ceff/(Q + Ceff)) * If(i);

end

c = vect;
```

BIBLIOGRAPHY

1) Carlson, R. W., & Sikic, B. I. (1983). Continuous infusion or bolus injection in cancer chemotherapy. *Ann Intern Med*, *99*, 823–833. Retrieved from http://www.ncbi.nlm.nih.gov/pubmed/6197002

2) el-Kareh, A. W., & Secomb, T. W. (1997). Theoretical models for drug delivery to solid tumors. *Critical Reviews in Biomedical Engineering*, *25*, 503–571. doi:10.1615/CritRevBiomedEng.v25.i6.20

3) El-Kareh, A. W., & Secomb, T. W. (2003). A Mathematical Model for Cisplatin Cellular Pharmacodynamics1. *Neoplasia (New York, N.Y.)*, *5*, 161–169.

4) Howlader, N., Noone, A. M., Krapcho, M., Neyman, N., Aminou, R., & Waldron, W. (2011). SEER Cancer Statistics Review, 1975–2010, National Cancer Institute. Bethesda, MD, based on November 2012 SEER data submission, posted to the SEER web site, 2013. *http://seer.cancer.gov/csr/1975_2010 (Accessed on June 08, 2013).*

5) Jones, L. B., Secomb, T. W., Dewhirst, M. W., & El-Kareh, A. W. (2014). The additive damage model: A mathematical model for cellular responses to drug combinations. *Journal of Theoretical Biology*, 1–11. doi:10.1016/j.jtbi.2014.04.032

6) Kolodziej, M., Hoverman, J. R., Garey, J. S., Espirito, J., Sheth, S., Ginsburg, A., … Beveridge, R. (2011). Benchmarks for Value in Cancer Care: An Analysis of a Large Commercial Population. *Journal of Oncology Practice*. doi:10.1200/JOP.2011.000394

7) Less, J. R., Skalak, T. C., Sevick, E. M., & Jain, R. K. (1991). Microvascular architecture in a mammary carcinoma: branching patterns and vessel dimensions. *Cancer Research*, *51*, 265–273.

8) Levasseur, L. M., Slocum, H. K., Rustum, Y. M., & Greco, W. R. (1998). Modeling of the time-dependency of in vitro drug cytotoxicity and resistance. *Cancer Research*, *58*, 5749–5761.

9) Lin, J. H., & Lu, A. Y. (1997). Role of pharmacokinetics and metabolism in drug discovery and development. *Pharmacological Reviews*, *49*, 403–449.

10) Minchinton, A. I., & Tannock, I. F. (2006). Drug penetration in solid tumours. *Nature Reviews. Cancer*, *6*, 583–592. doi:10.1038/nrc1893

11) Nagai, N., & Ogata, H. (1997). Quantitative relationship between pharmacokinetics of unchange cisplatin and nephrotoxicity in rats: Importance of area under the concentration-time curve (AUC) as the major toxicodynamic determinant in vivo. *Cancer Chemotherapy and Pharmacology*, *40*, 11–18. doi:10.1007/s002800050618

12) Perrin, S. (2014). Make mouse studies work. *Nature*, *507*, 423. doi:10.1038/507423a

13) Takimoto, C. H. (2009). Maximum tolerated dose: Clinical endpoint for a bygone era? *Targeted Oncology*. doi:10.1007/s11523-009-0108-y

14) Tang, L., Van De Ven, A. L., Guo, D., Andasari, V., Cristini, V., Li, K. C., & Zhou, X. (2014). Computational modeling of 3D tumor growth and angiogenesis for chemotherapy evaluation. *PLoS ONE*, *9*. doi:10.1371/journal.pone.0083962

15) Toley, B. J., Tropeano Lovatt, Z. G., Harrington, J. L., & Forbes, N. S. (2013). Microfluidic technique to measure intratumoral transport and calculate drug efficacy shows that binding is essential fMicror doxorubicin and release hampers Doxil. *Integrative Biology*, *5*, 1184–1196. doi:10.1039/c3ib40021b

16) Tredan, O., Galmarini, C. M., Patel, K., & Tannock, I. F. (2007). Drug resistance and the solid tumor microenvironment. *J Natl Cancer Inst*, *99*, 1441–1454. doi:10.1093/jnci/djm135

17) Venkatasubramanian, R., Henson, M. A., & Forbes, N. S. (2008). Integrating cell-cycle progression, drug penetration and energy metabolism to identify improved cancer therapeutic strategies. *Journal of Theoretical Biology*, *253*, 98–117. doi:10.1016/j.jtbi.2008.02.016